Finger Probe Array for Topography-Tolerant Scanning Electrochemical Microscopy of Extended Samples

- Electronic supporting information –

Andreas Lesch,[†,‡,#] Po-Chung Chen,[†,§,#] Folkert Roelfs,[†] Carsten Dosche,[†] Dmitry Momotenko,[‡] Fernando Cortés-Salazar,[‡] Hubert H. Girault[‡] and Gunther Wittstock[†,*]

[†] Carl von Ossietzky University of Oldenburg, School of Mathematics and Natural Sciences, Center of Interface Science, Department of Chemistry, D-26111 Oldenburg, Germany

[‡] Ecole Polytechnique Fédérale de Lausanne, Laboratoire d'Electrochimie Physique et Analytique, Station 6, CH-1015 Lausanne, Switzerland

[#] A.L. and P.-C.C. contributed equally.

[§] Present address: Institute of Systems Biology and Bioinformatics, National Central University; No. 300, Jhongda Rd., Jhongli City, Taoyuan County 32001, Taiwan (R.O.C.)

[*] CORRESPONDING AUTHOR FOOTNOTE

EMAIL: gunther.wittstock@uni-oldenburg.de

Telephone number: +49(0)-441-798-3971

Fax number: +49(0)-441-798-3979

SI-1: Radii, *RG* values and working distances in contact mode of the used microelectrodes

Table S-1. Microdisk radii r_T, glass sheath radii r_{glass}, *RG* values and calculated working distances *d* of MEs 1 to 4 of the FPMEA.

k	1	2	3	4
r_T / µm [a]	11.9	12.9	11.9	12.4
r_{glass} / µm [b]	123.8	108.4	135.7	136.4
RG [b]	10.4	8.4	11.4	11.0
d (h_P = 0 µm) / µm [c]	21.5	18.8	23.6	23.7

[a] determined by chronoamperometry in 4 mM $K_4[Fe(CN)_6]$ and 0.1 M KCl with $D = 0.65 \cdot 10^{-5}$ cm^2 s^{-1}.

[b] determined by CLSM. [c] Calculated from geometric considerations.

Table S-1 contains the microdisk radii r_T, the radii r_{glass} of the insulating glass sheaths and the *RG* values ($RG = r_{glass}/r_T$) of the microelectrodes (MEs) used in the presented work. Furthermore, it shows calculated working distances *d* in contact mode on the basis of the geometric considerations made in SI-2.

SI-2: Definition of h_P

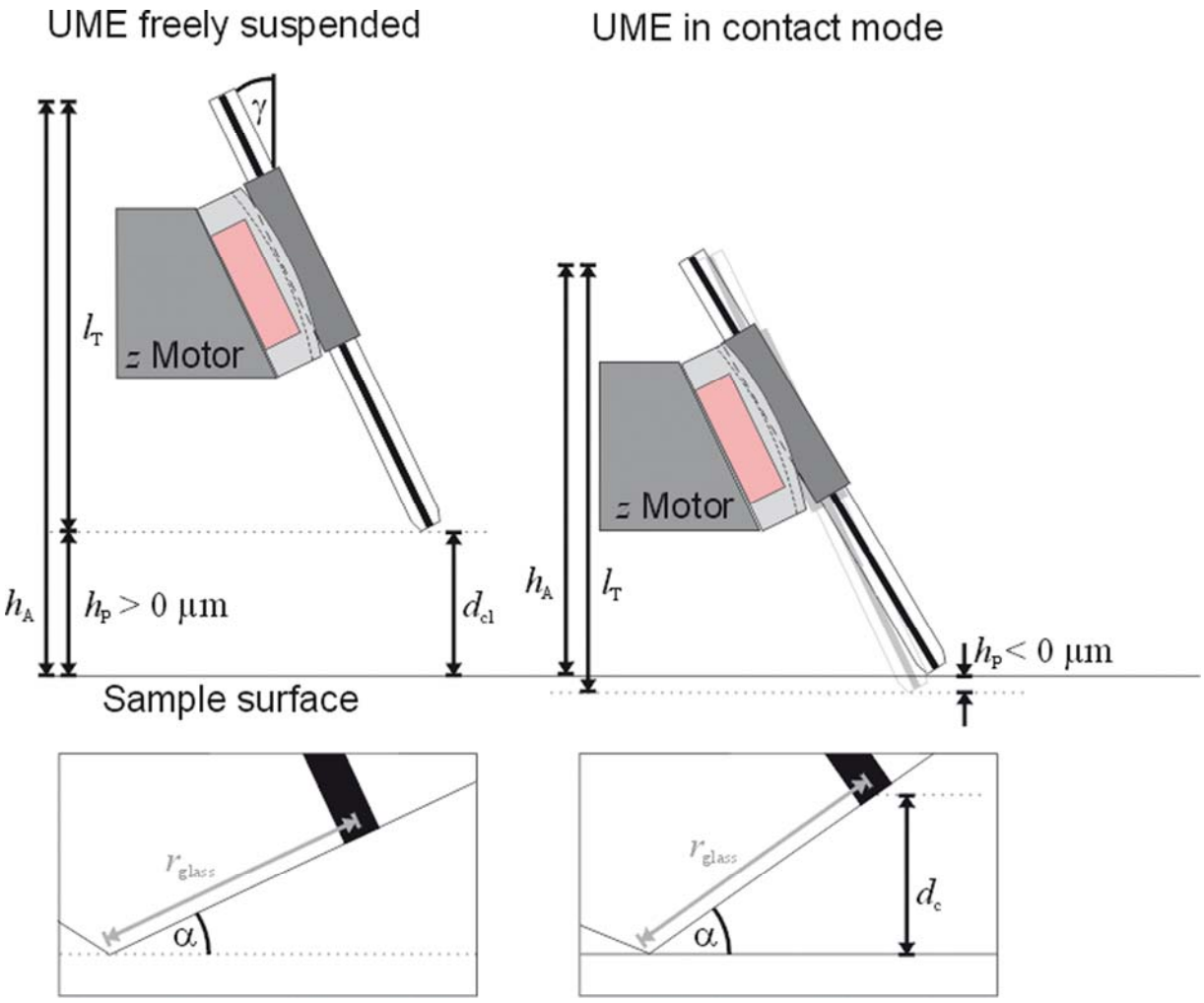

Figure S-1. Schematic representation of one ME of the finger probe array mounted in the custom-made SECM holder for vertical approaching. Left panel: Situation when the ME is freely suspended in bulk solution. Right panel: Situation after mechanical contact of the ME and sample.

Figure S-1 shows the geometric arrangements of one ME of the ME finger probe array during vertical positioning. The concept is based on the geometric considerations previously made for the soft SECM probes. The MEs are approached to a surface under an inclination angle γ, usually between 10° and 20°. This inclination angle ensures sliding of the ME in the desired horizontal direction after it has been brought into mechanical contact with the substrate. A vertical length l_T

of the ME and a height of the attachment point above the sample h_A were defined (left panel in Figure S-1). The vertical difference between these two points is used to calculate the important quantity h_P.

$$h_P = h_A - l_T \quad \text{(S-2.1)}$$

As can be seen in the right panel, h_P becomes negative when the ME continues vertical approaching after the mechanical contact between the glass sheath of the ME and the substrate has been made. α represents the angle between the probe surface including the Pt disk ME and the horizontal which is equal to the sample surface. This angle continuously increases when the ME slides on the surface during vertical approaching. The effective working distance d_{eff} in contact and contactless mode (index c and cl, respectively) can be calculated using the following equations:

$$\text{cl: } d_{eff,cl} = r_{glass} \cdot \sin \alpha + h_P;\ h_P > 0 \quad \text{(S-2.2)}$$

$$\text{c: } d_{eff,c} = r_{glass} \cdot \sin \alpha;\ h_P < 0 \quad \text{(S-2.3)}$$

During vertical scanning the probes are translated from right to left.

SI-3: Stability of the position of the MEs in the new probe holder

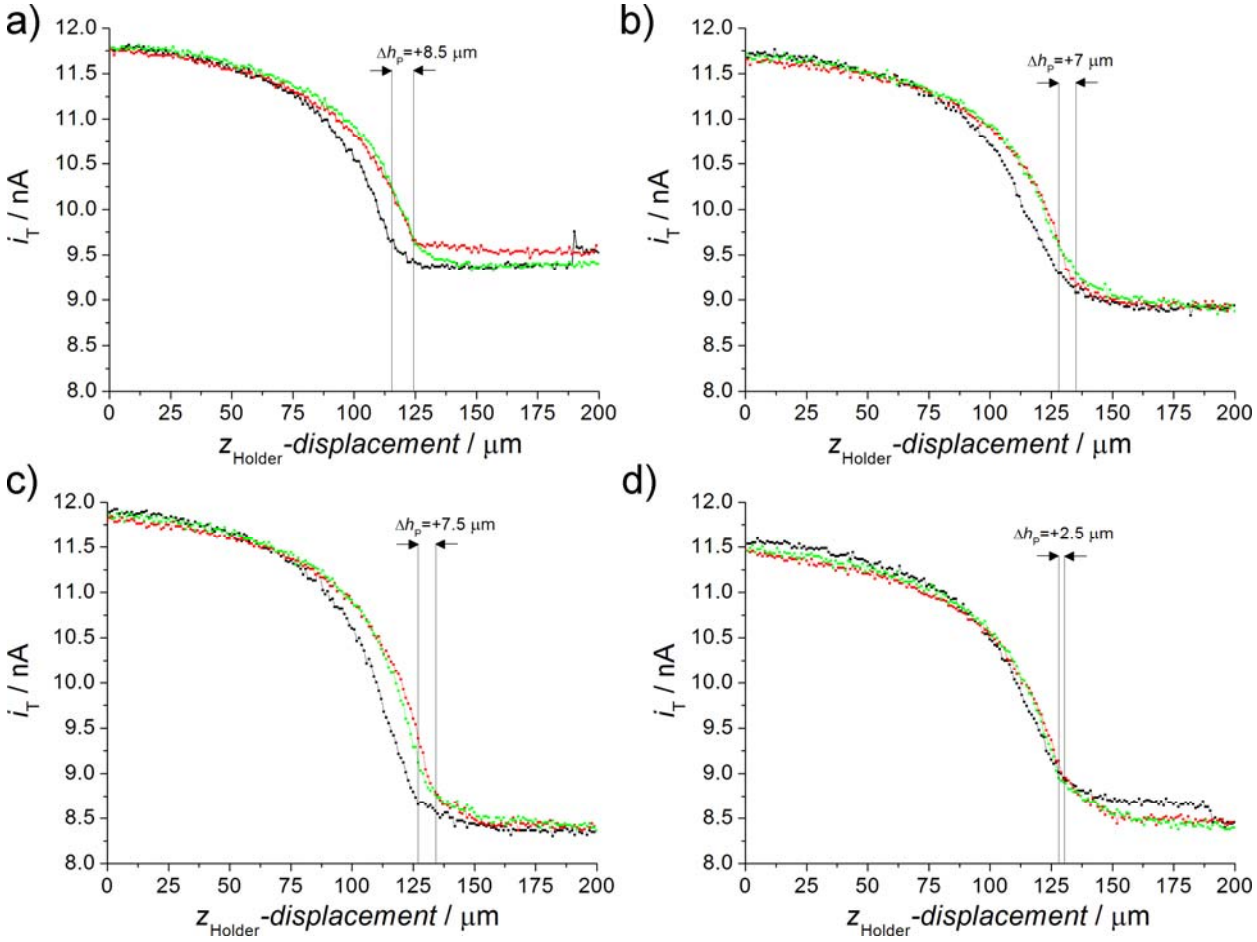

Figure S-2. Behavior of four MEs (a-d) of a finger prober array during approaching (black curve), retracting (red) and re-approaching (green). Vertical displacement of the individual MEs in a finger probe array was 200 µm. Translation rate 1 µm s^{-1}, step size 1 µm. Electrolyte solution: 4 mM $K_4[Fe(CN)_6]$ in 0.1 M phosphate buffer (pH 7.0). The z_{Holder}-*displacement* represents the vertical translation of the complete holder towards the sample. Vertical lines represent the *z*-position, at which the individual MEs came in mechanical contact with the PI substrate and started to slide.

The stability of the position of the MEs in the holder during repetitive approach curves was investigated by performing a first approach curve (black curve in Figure S-2), a retract curve (red curve) and a re-approach curve (green) using the same vertical distance of 200 µm for all three experiments. A vertical shift of the h_P value (Δh_P) due to slight sliding of the MEs in the holder

between the first (black) and second approach curve (green) is indicated for ME 1 (a, Δh_P = +8.5 µm), ME 2 (b, Δh_P = +7 µm), ME 3 (c, Δh_P = +7.5 µm) and ME 4 (d, Δh_P = +2.5 µm). There is a slight shift of the MEs in the holder during first approach curves. The steel tubes move slightly up which results in a shift of the ME on the sample of h_P < 8 µm. However, after repetitive approach curves a steady-state situation is achieved and imaging can be performed without further shifts as can be seen in the feedback image of one exemplary ME in Figure S-3. This is also confirmed by the feedback images in the main manuscript.

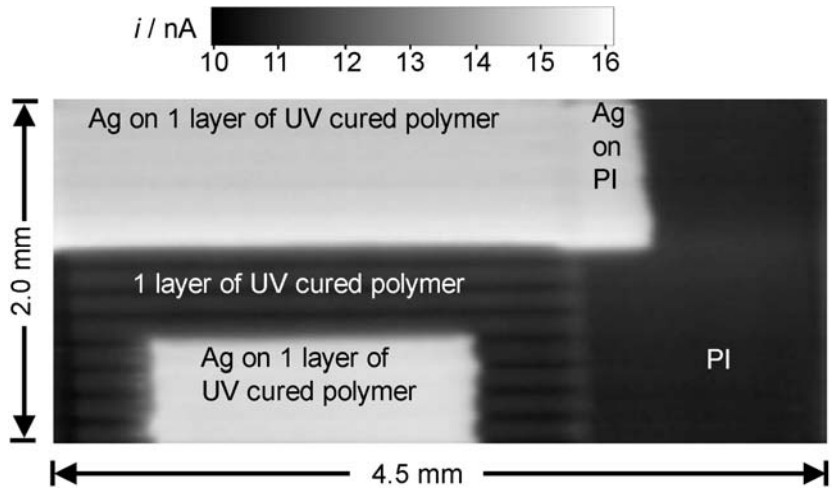

Figure S-3. SECM feedback image taken with one ME of the finger probe array. Experimental conditions: Step size = 25 µm, translation rate = 25 µm s^{-1}. Electrolyte solution 4 mM $K_4[Fe(CN)_6]$ in 0.1 M phosphate buffer (pH 7.0), E_T = 0.3 V. h_P = -38 µm. Lift off height = 200 µm.

SI-4: Estimation of the force exerted by the MEs of the finger probe array on the surface

An analytical balance (CP 124 S, Sartorius, Göttingen, Germany) measured the force exerted by the FPMEA when brought into mechanical contact with a sample placed on top of the balance.[1] Firstly, the array was mounted on the custom-built holder with an inclination angle of 10° and a PI substrate was mounted to the plate of the analytical balance. Then, the ME was approached from air to the PI surface and the measured masses for four vertical displacements h_p were recorded. Multiplication of the masses with the gravity constant (g = 9.81 m s^{-2}) gives the estimated force. The force *vs.* the displacement is plotted in Figure S-4. Linear regression through zero gives

$$F(h_P) = -k_{Spring} \cdot h_P = -0.64 \text{ mN } \mu m^{-1} \cdot h_P \quad \text{(S-4.1)}$$

where k_{Spring} is the slope and represents the spring constant of the ME in the magnet-based holder. In case of a displacement h_P = -20 µm:

$$F = 0.64 \text{ mN } \mu m^{-1} \cdot 20 \text{ µm} = 12.8 \text{ mN} \quad \text{(S-4.2)}$$

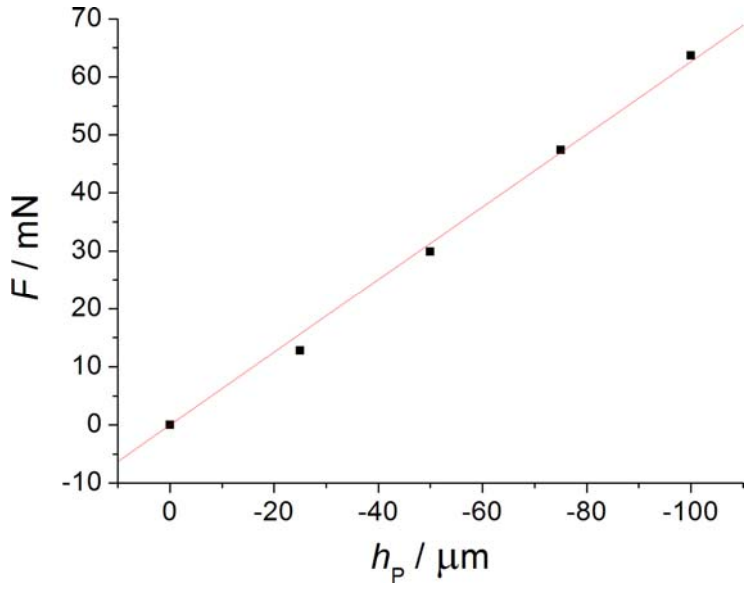

Figure S-4. *F vs*. the ME displacement during approach curves towards the sample surface after the point of mechanical contact of the ME with the substrate.

SI-5: Inkjet-printed 3D sample

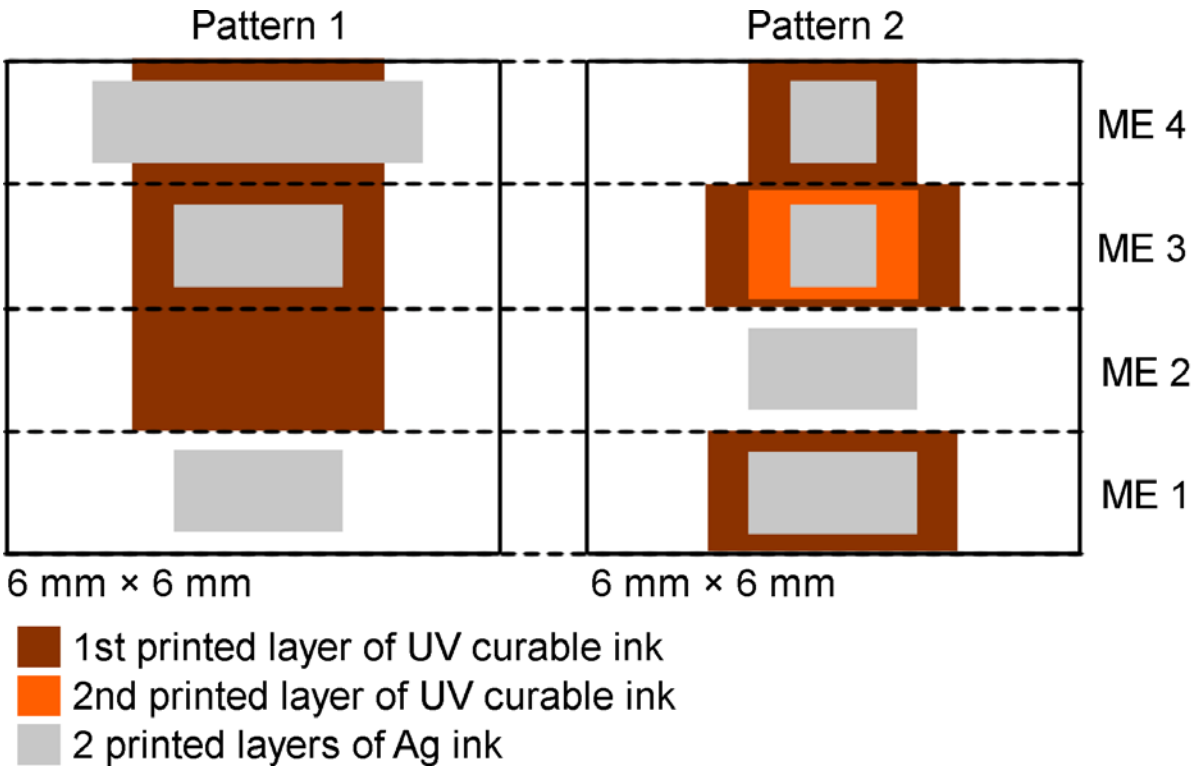

Figure S-5. Design of the 3D structure developed for experiments using the ME finger probe array consisting of four MEs.

A 3D sample was specially designed for demonstrating the topography-tolerant scanning of the ME finger probe array (Figure S-5). The sample consists of two main patterns each 6 mm × 6 mm in size. Each of these two patterns includes four areas to be scanned by the four MEs of the finger probe array (indicated by dashed lines). The support material is a 125 µm thick PI sheet. In order to obtain a 3D structure, a UV curable ink was inkjet-printed and simultaneously UV-cured. Figure S-6 shows two height profiles of the inkjet-printed patterns 1 (a) and 2 (b) recorded with the DektakXT mechanical profiler (Bruker, Billerica, USA). The profiles were recorded in the vertical center of the patterns and from bottom to top with respect to the schematic representation of the sample in Figure S-5. As can be seen, the UV-cured polymer represents a waved shape. This is due to the simultaneous inkjet-printing and UV curing process. Each of

these waves represents one printed band of UV-cured polymer using 3 nozzles. A first layer printing of UV curable ink resulted in a pattern with a maximum height of 4 µm. A step height of 12-13 µm was achieved with a second layer printing of the UV-cured polymer using a smaller drop spacing to deposit a larger volume per area. Therefore, the width of the bands is smaller than in the first layer. Two layers of Ag were printed on top of the PI and on the UV-cured polymer resulting in an additional height of approx. 1.5 µm.

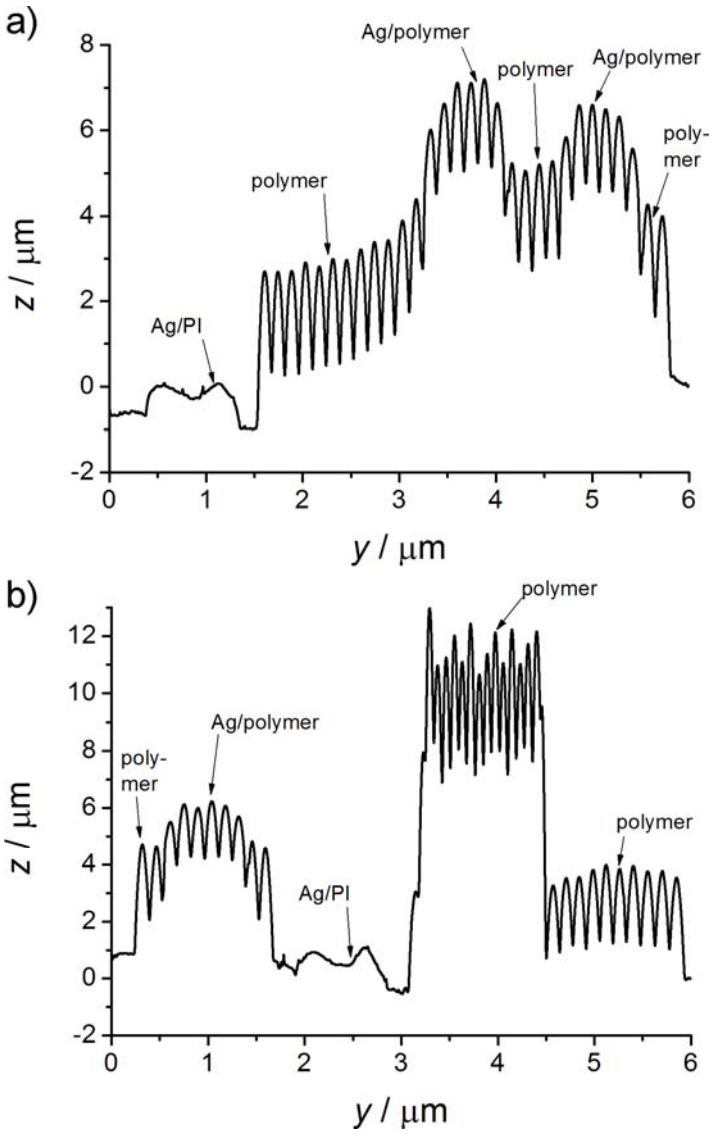

Figure S-6. Height profiles of pattern 1 (a) and pattern 2 (b) measured by mechanical profilometry.

SI-6: SECM imaging of inkjet-printed 3D sample by using soft linear arrays of microelectrodes

For comparison, the 3D structure was investigated by using soft linear microelectrode arrays (SLMEAs) in contact mode imaging. For details of these probes, the reader is invited to read our previous publications about this topic.[1-5] In the following, a brief overview about experimental details is given followed by a short discussion.

Chemicals. Ferrocenemethanol (FcMeOH; ≥97%; Sigma–Aldrich, Buchs, Switzerland) and potassium chloride (KCl; Sigma–Aldrich, Buchs, Switzerland) were used as received. Deionized water was produced by a Purelab® Classic (Elga LabWater, United Kingdom) and a Milli-Q plus 185 model (Millipore, Zug, Switzerland).

Fabrication of soft linear carbon microelectrode arrays. Carbon SLMEAs were prepared as previously reported.[3, 5, 6] In brief, microchannels with a midpoint-to-midpoint distance of 500 µm were UV laser-ablated (193 nm ArF excimer laser; fluence = 250–350 mJ; frequency = 50 Hz; LambdaPhysik, Göttingen, Germany) through a metallic mask into 100 µm thick PET foils (PET; Melinex Dupont, Wilmington, USA). The average length, width and depth of the prepared microchannels were 6 cm, 30 µm and 20 µm, respectively. After filling with the Electrador carbon ink (Electra Polymer & Chemicals Ltd., Roughway Mill, Dunk Green, England), electrical conductivity of the carbon tracks was achieved by curing for 1 h at 80 °C. The carbon tracks were covered and sealed with a 3-5 µm thick layer of Parylene C (Comelec SA Parylene depositioning system, La Chaux-de-Fonds, Switzerland). The active electrode areas were defined by the cross-section which was exposed by razor blade cutting. Carbon MEs with the shape of slightly distorted sickles were obtained.

SECM experiments. The same setup was used as described in the main manuscript except the array holder. For the SLMEAs, the holder for soft probes was used as described in detail in ref. [4].

FcMeOH was used as redox mediator and a potential of E_T = 0.4 V was applied to all carbon MEs. Imaging was performed as for the FPMEA in the main manuscript, *i.e.* usage of a lift off mode during array repositioning. Due to slight variations in sizes, geometries and working distances of the individual MEs of SLMEAs, the currents vary slightly between the individual MEs as the ones for the FPMEA. The same calibration routine as described in the main manuscript was applied.

SECM imaging of large and complex 3D samples using a soft linear microelectrode array

High-throughput feedback mode imaging of the 3D structure was performed using a soft linear array of eight carbon microelectrodes. The image is shown in Figure S-7. The multiple image procedure was applied which was introduced previously[3] after aligning the array to the sample surface using the worm gear of the SECM holder[4] and after approaching it to h_P = -81 µm on the PI substrate ensuring a probe-sample contact during imaging. The HF scanning direction was from right to left. The image covered an area of 4.5 mm × 8 mm of the sample. With a step size of 20 µm in HF as well as in LF direction, each ME of the SLMEA scanned 480 µm in *y*-direction until the MEs would scan an area that has already been investigated by the adjacent electrode (electrode separation was 500 µm, the frame size in LF direction was 3980 µm). At this point of the experiment, the SLMEA was translated by a large step of 4000 µm in the LF direction onto the contiguous sample region followed by recoding a second image and combining the image frames automatically into a single data set (Figure S-7a). The image acquisition took 4 h 42 min for 90400 grid points (point density = 2511 mm^{-2}).

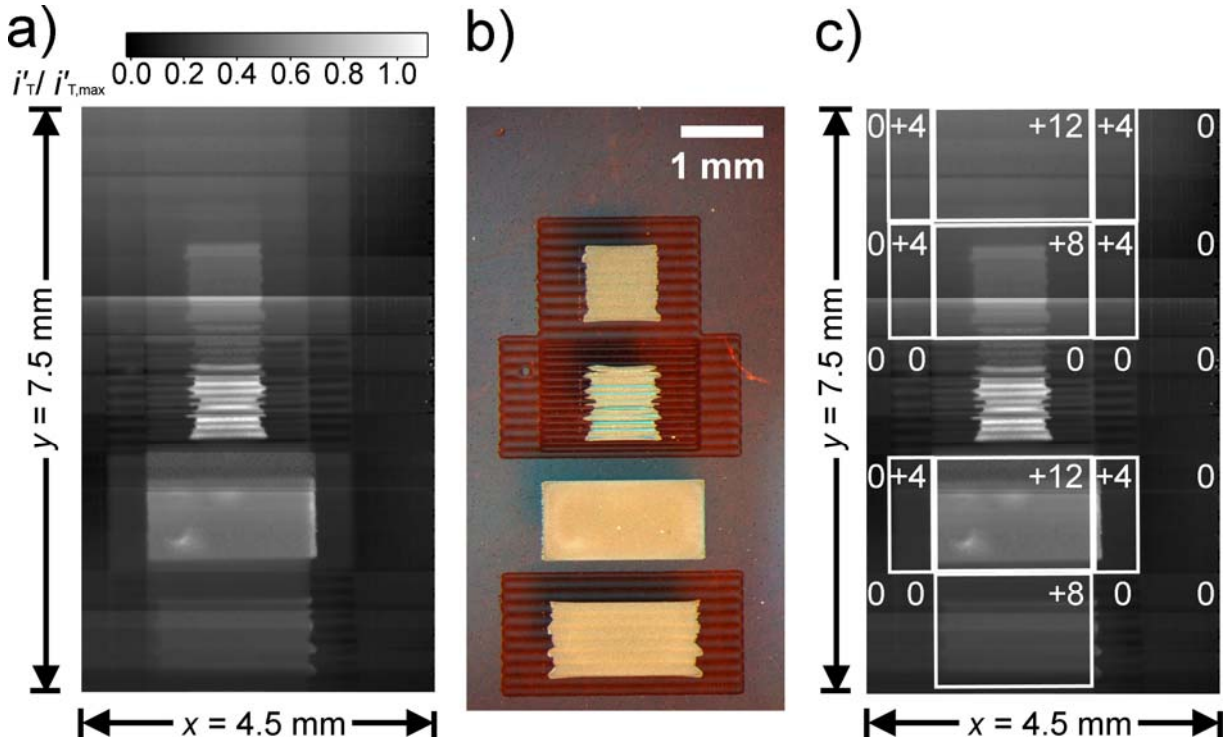

Figure S-7. SECM feedback mode imaging of the 3D sample using a carbon SLMEA of 8 MEs. a) transformed SECM image. Experimental conditions: 2 mM FcMeOH + 0.1 M KCl. E_T = 0.4 V. h_P = -81 µm, LO stroke height 350 µm, LO retract speed 400 µm s^{-1}, LO approach speed 10 µm s^{-1}, HF fwd step size 20 µm, HF $v_{T,fwd}$ = 25 µm s^{-1}, HF rev step size 20 µm, HF $v_{T,rev}$ = 1000 µm s^{-1}, LF fwd step size 20 µm, LF $v_{T,fwd}$ = 25 µm s^{-1}, LF large step 4000 µm; b) Photograph of the scanned pattern *after* the experiments taken with a Nikon D50 DSLR digital camera (Nikon, Tokyo, Japan). c) SECM image with estimated changes of working distance Δd in µm compared to the situation with h_P = -81 µm.

Imaging could be performed without tilt correction and without paying attention to the topography. The individual responses of the eight MEs were transformed using the calibration values listed in Table S-2 and were plotted as $i'_{T,k}/i'_{T,max.k}$. The conducting and insulating sample regions can be easily identified. Since the cross-section of the UV-cured polymer structures of the sample were waved, the working distance in the ditches of the UV-cured polymer is slightly larger, hence the waves of the printed polymer structure are identifiable. The comparison of the

feedback image with the optical micrograph (Figure S7-b, taken *after* the experiments) showed that the entire SLMEA body is lifted since the entire probe follows the profile of the highest topographic structures. Only in these highest regions of the sample, the working distances of the respective MEs remained constant and provided image data with high resolution (central region of images in Figure S-7a and c). The approximate variation of the working distances Δd for the different sample regions were labeled in Figure S-7c. For instance, due to the first two insulating patterns of about 4 µm height, the microelectrodes that are located on these stairs still show very similar hindered diffusion owing to a constant working distance (Δd = 0 µm). For the other electrodes, the Parylene C coating side lost mechanical contact to the PI (Δd = +4 µm) which caused a significant increase in the current for hindered diffusion. The UV-cured polymer in the middle of the *y*-direction in Figure S-7c was approximately 12 µm high with respect to the PI substrate. Over this region, the MEs were close to the substrate and for this region image data show high resolution and good current contrast. At these *x*-positions, Δd was approximately +12 µm and +8 µm for the other MEs which caused an additional increase of the measured current for hindered diffusion. Although the working distance increased for some MEs, the Ag pattern on the PI can easily be identified. Please note that the SLMEA was slightly pressed onto the sample and hence it will bend along the probe width which might decrease the working distances slightly. It has to be pointed that imaging did not damage the printed Ag or polymer surfaces. The SLMEA itself remained intact and provided constant signals over the whole measurement period. However, these results demonstrate the need of the FPMEA as presented in the main manuscript.

The scheme in Figure S-8a demonstrates the behavior of the soft probe array in contact mode at six different positions. At the starting point of the two images (x = 0.0 mm) the entire edge of the

soft probe including the Parylene C coating and the microelectrodes is in contact with the sample. At x = 1.3 mm the entire probe has climbed on the two stairs of about 4 µm in height. Therefore, the working distances of some microelectrodes enlarge. At x = 3.0 mm the soft probe has been moved up further due to the height of the substrate feature of about 12 µm. As can be seen in the third line in Figure S-8a, the largest topographic feature is at the edge of the soft probe before as well as after the large step. Due to the pressure which is exerted by the soft probe onto the sample, the probe bends additionally approaching the freely suspending working electrodes.

Figure S-8b shows the two recorded image regions in the multiple imaging routine where the red square shows the scanned areas of the first image and the blue one of the second image after a large step of 4000 µm in the LF (y-) direction.

Table S-2 contains the applied correction values of the SECM image.

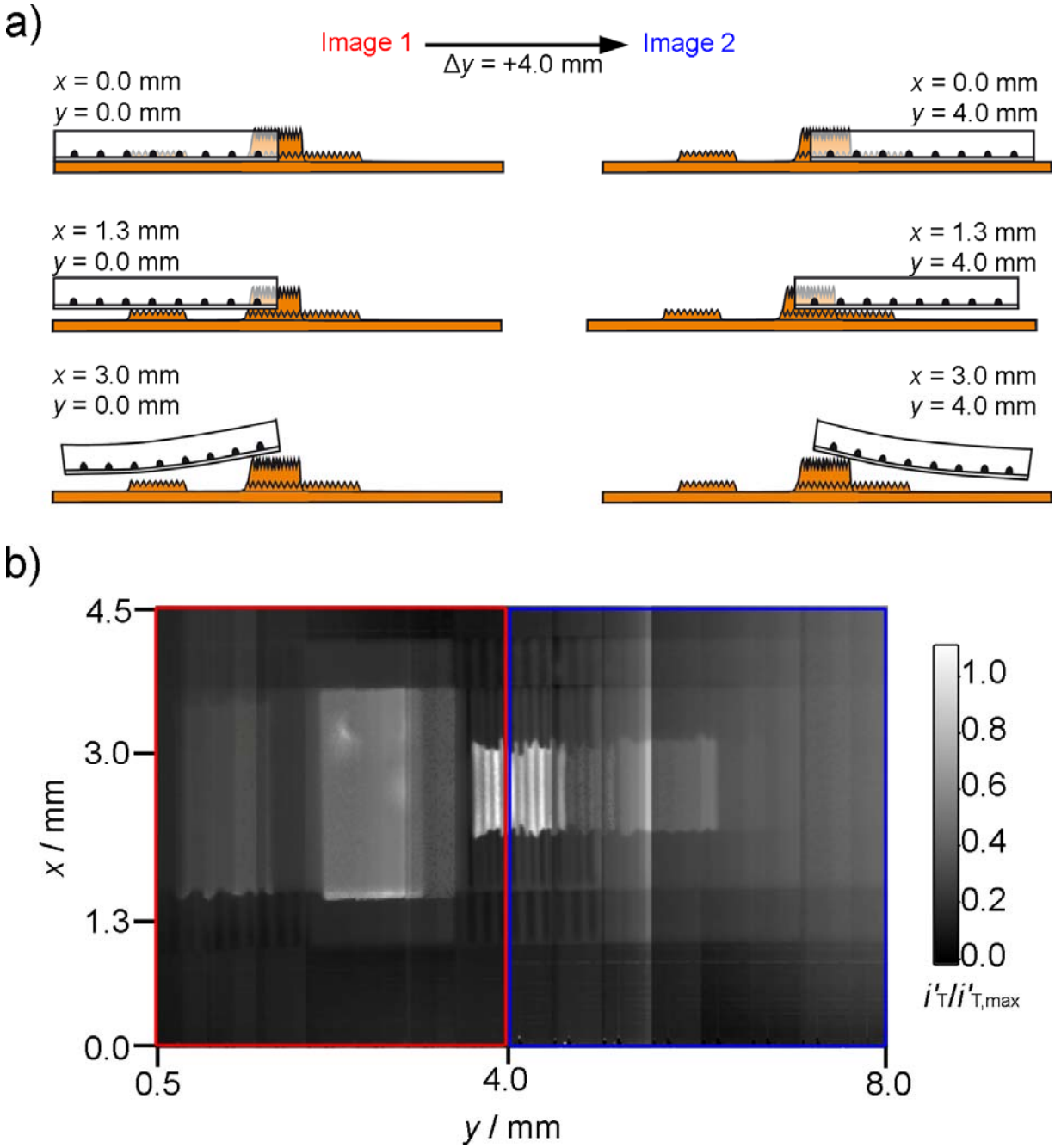

Figure S-8. SECM imaging of the 3D sample structure by using a soft linear array of eight carbon microelectrodes. a) Schematic representation of the array when the entire probe body is in mechanical contact with the substrate (no topography; x = 0.0 mm) and when the entire body is lifted off following the highest topographic artifacts (e.g. x = 3.0 mm). b) SECM feedback mode image. Image 1 (red) and image 2 (blue) of the two-step multiple image experiment are indicated by colored rectangles.

Table S-2. Positional offsets $x_{off,k}$ and $y_{off,k}$, current offsets $i_{T,off,k}$ and scale factors s_k applied in Figure S-7a.

k	1	2	3	4	5	6	7	8
$x_{off,k}$ / μm	0	0	0	0	0	0	0	0
$y_{off,k}$ / μm	0	500	1000	1500	2000	2500	3000	3500
$i_{T,off,k}$ / nA[a]	2.393 (1.900)	1.904	1.908	2.273	3.193	3.245	2.43	2.295 (2.5)
s_k / nA^{-1} [a]	0.075	0.075	0.164	0.071	0.09	0.08	0.11	0.053 (0.8)

[a] the values in brackets indicate adjusted values in the 2nd image of the two-step multiple image.

SI-7: Positional offsets, current offsets and scale factors applied in the FPMEA image

The original image frames of the four MEs of Figure 3 in the main manuscript are shown in Figure S-9. Imaging conditions: solution of 4 mM $K_4[Fe(CN)_6]$ and 0.1 M phosphate buffer (pH 7.0), E_T = 0.3 V, sample at open circuit potential, h_P values: -25 µm (ME 1), -32.5 µm (ME 2), -23 µm (ME 3), -50.5 µm (ME 4). LO stroke height 200 µm, LO retract speed 25 µm s^{-1}, LO approach speed 25 µm s^{-1}, HF fwd step size 25 µm, HF $v_{T,fwd}$ = 25 µm s^{-1}, HF rev step size 25 µm, HF $v_{T,rev}$ = 25 µm s^{-1}, LF fwd step size 25 µm, LF $v_{T,fwd}$ = 25 µm s^{-1}.

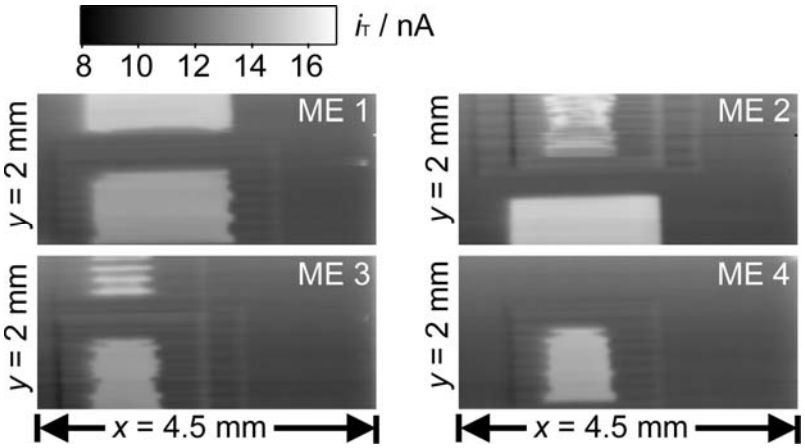

Figure S-9. Original SECM image frames of the four MEs of Figure 3 in the main manuscript.

Table S-3. Positional offsets $x_{off,k}$ and $y_{off,k}$, current offsets $i_{T,off,k}$ and scale factors s_k applied in Figure 3 in the main manuscript. In addition, the steady-state currents $i_{T,\infty,k}$ of the MEs in bulk solution are listed.

k	1	2	3	4
$x_{off,k}$ / µm	0	66	-310	125
$y_{off,k}$ / µm	0	1798	3090	4477
$i_{T,off,k}$ / nA	10.344	10.22	9.896	10.251
s_k / nA^{-1}	0.194	0.166	0.194	0.231
$i_{T,\infty,k}$ / nA	12.47	13.02	12.36	12.68

SI-8: Current calibration vs current normalization

In order to demonstrate the limitation of applying normalized currents $I_T = i_{T,k}/i_{T,\infty,k}$ compared to calibrated currents $i'_{T,k}/i'_{T,max,k}$, the original currents $i_{T,k}$, the normalized currents and the calibrated currents of three simultaneously recorded, exemplary line scans using three different MEs of a FPMEA are shown in Figure S-10.

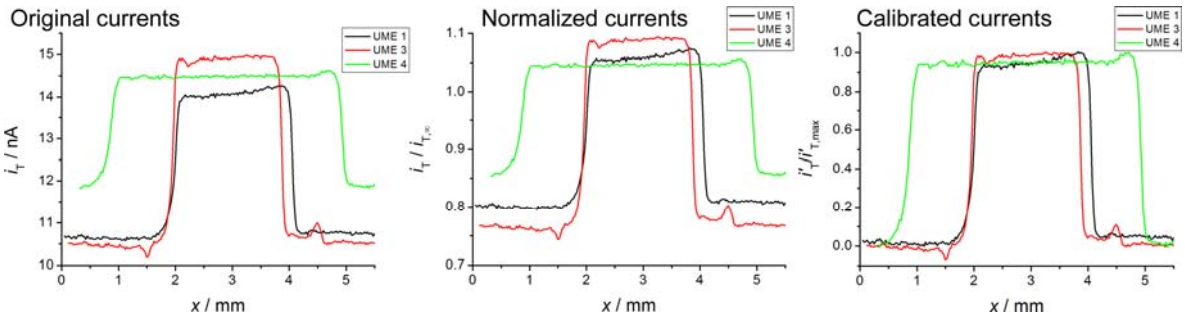

Figure S-10. Original currents, normalized currents and calibrated currents of three simultaneously recorded line scans in contact mode using the FPMEA above a silver on polymer structure.

Table S-4 shows the measured steady-state currents $i_{T,\infty,k}$ and the calibration values to get $i'_{T,k}/i'_{T,max,k}$.

Table S-4. Steady-state currents, current offsets and scale factors used in Figure S-10.

k	1	3	4
$i_{T,\infty,k}$ / nA	13.30	13.70	13.85
$i_{T,off,k}$ / nA	10.58	10.50	11.84
s_k / nA^{-1}	0.27	0.22	0.36

From Figure SI-10 it is evident, that current normalization $i_{T,k}/i_{T,\infty,k}$ does not result in equivalent currents above insulators and conductors for all participating electrodes whereas the calibration $i'_{T,k}/i'_{T,max,k}$ yields equal current responses for all three MEs. Therefore, a calibration is applied for Figure 3 in the main manuscript. However, we would like to emphasize that our high-

throughput contact-mode imaging concept is not intended for extracting quantitative kinetic data. It was developed for reactivity imaging. Therefore, the SLMEAs as well as the FPMEAs should not be applied for quantitative kinetic studies.[1]

REFERENCES

(1) Lesch, A.; Momotenko, D.; Cortes-Salazar, F.; Wirth, I.; Tefashe, U. M.; Meiners, F.; Vaske, B.; Girault, H. H.; Wittstock, G. *J. Electroanal. Chem.* **2012**, *666*, 52-61.

(2) Cortes-Salazar, F.; Momotenko, D.; Girault, H. H.; Lesch, A.; Wittstock, G. *Anal. Chem.* **2011**, *83*, 1493-1499.

(3) Cortes-Salazar, F.; Momotenko, D.; Lesch, A.; Wittstock, G.; Girault, H. H. *Anal. Chem.* **2010**, *82*, 10037-10044.

(4) Lesch, A.; Momotenko, D.; Cortés-Salazar, F.; Roelfs, F.; Girault, H. H.; Wittstock, G. *Electrochim. Acta* **2013**, *110*, 30-41.

(5) Lesch, A.; Vaske, B.; Meiners, F.; Momotenko, D.; Cortes-Salazar, F.; Girault, H. H.; Wittstock, G. *Angew. Chem. Int. Ed.* **2012**, *51*, 10413-10416.

(6) Cortes-Salazar, F.; Träuble, M.; Li, F.; Busnel, J.-M.; Gassner, A.-L.; Hojeij, M.; Wittstock, G.; Girault, H. H. *Anal. Chem.* **2009**, *81*, 6889-6896.